

Research Article

Nonminutiae-Based Decision-Level Fusion for Fingerprint Verification

Sadegh Helfroush and Hassan Ghassemian

Department of Electrical Engineering, Tarbiat Modares University, P.O. Box 14115-111, Tehran 1411713116, Iran

Received 19 April 2006; Revised 20 September 2006; Accepted 20 September 2006

Recommended by Mark Liao

Most of the proposed methods used for fingerprint verification are based on local visible features called *minutiae*. However, due to problems for extracting minutiae from low-quality fingerprint images, other discriminatory information has been considered. In this paper, the idea of decision-level fusion of *orientation*, *texture*, and *spectral* features of fingerprint image is proposed. At first, a value is assigned to the similarity of block orientation field of two-fingerprint images. This is also performed for texture and spectral features. Each one of the proposed similarity measure does not need core-point existence and detection. Rotation and translation of two fingerprint images are also taken into account in each method and all points of fingerprint image are employed in feature extraction. Then, the similarity of each feature is normalized and used for decision-level fusion of fingerprint information. The experimental results on *FVC2000* database demonstrate the effectiveness of the proposed fusion method and its significant accuracy.

Copyright © 2007 Hindawi Publishing Corporation. All rights reserved.

1. INTRODUCTION

Lots of efforts have been made on fingerprint verification. Most of them have focused on extracting and matching local visible features of fingerprint image called minutiae [1–3]. Fingerprint preparation for minutiae extraction needs several complex steps [4, 5]. These time-consuming steps are fingerprint enhancement, directional filtering, segmentation, and thinning. They may erroneously introduce false minutiae and reject some real minutiae points. Therefore, some additional steps must be provided to alleviate these errors. In addition, it is hardly possible for low-quality images to reliably extract minutiae points and a complementary matching method is needed for low-quality fingerprint verification.

There are a limited number of verification methods that do not use minutiae points for matching. They are called image-based approaches. They extract features for matching by applying a certain type of filter banks or using special transformations. They have the advantage of lower computational complexity over the minutiae-based methods so that the verification speed of these methods will be significant. However, they suffer from lower accuracy. Besides, the existence and detection of a reference point (usually core point) in the captured fingerprint area are crucial for most of image-

based systems. Although different fingerprints have discriminatory information around the core point, it is better to examine other areas of fingerprint image for such information. When the core point cannot be reliably detected or it is close to the border of fingerprint area, the extracted features of input fingerprint may be incomplete or incompatible with respect to the template. In [6], a wavelet-based fingerprint recognition method has been presented. This method has been applied on a small database. In addition, recognition rate is improved with an increase in number of fingerprint images stored in database per user, and hence, larger memory size is needed for performance improvement. In [7], verification is achieved using the features extracted by applying eight Gabor filters around the core point. Two alterations of [7] are presented in [8, 9]. In [8], at first, a subsampling at the block level is performed on fingerprint image to improve the efficiency and then, Gabor filters are applied. In [9], instead of storing the response of each filter at each sampling point, only the index of the filter with the highest response is used for fingerprint matching. In [10], the features are extracted using directional filter bank. This method is too complex and the values reported for the system evaluation are unsatisfactory for a practical verification system. A fingerprint verification system based on the correlation of fingerprints is proposed in [11]. Rotation of fingerprints is not included in

this approach which may increase the computational complexity.

In [12], a verification method is proposed and it is based on the features extracted from Fourier-Mellin transform of fingerprint image around the core point. Also, the identification system proposed in [13] is based on Fourier-Mellin transform as the preprocessing step followed by a neural network as an identifier. In both [12, 13], it can be assumed that the features are extracted from the spectrum of fingerprint, as the features come from the spectrum of log-polar map of fingerprint spectrum. This point reveals that a verification system may be proposed and based on the features extracted from the spectrum. The advantages of using the spectrum for fingerprint verification are translation invariance property of spectrum and use of all points of fingerprint image in spectrum calculation. Obviously, due to the lack of phase information, spectrum-based verification may not be of high accuracy. However, the accuracy may be improved by the fusion with other kinds of features such as orientation or textural features.

There is discriminatory information found in orientation of fingerprint ridges that can be used for fingerprint verification [14, 15]. In [15], the best presented method uses the steepest descent algorithm for fingerprint registration and verification based on orientation field. The method heavily depends on the initial point selection.

Decision-level fusion of different verification methods is a challenge for performance improvement in fingerprint verification especially for low-quality images. In [16–18], matching systems are designed based on the fusion of minutiae points with the textural features extracted from Gabor filter bank. In [19], decision-level fusion of global orientation field with minutiae is used for fingerprint verification. In all presented fusion methods, there is an attempt to use minutiae features as a base for fusion [16–20]. On the other hand, it is almost impossible to extract minutiae for low-quality image. Therefore, a method of fusion may be proposed only based on nonminutiae features.

In this paper, we propose nonminutiae-based decision-level fusion for fingerprint verification using orientation, textural, and spectral features. Feature extraction in each case does not need a reference point. In addition, all points of fingerprint image are employed for feature extraction despite the presented methods that use only the points around the core.

This paper is organized as follows. In the following sections, methods for feature extraction and matching in orientation, textural, and spectral domains of fingerprint image are presented. Then, the normalization method is explained. Experimental results for the evaluation of the proposed method and decision-level fusion of features are given in Section 6. A brief conclusion section will summarize the paper.

2. SIMILARITY MEASURING USING BLOCK ORIENTATION FIELD (BOF)

The proposed method utilizes the likeness of BOFs for similarity measuring of two fingerprints. BOF is an image that

shows the dominant ridge orientation in a square block of original fingerprint image. In order to obtain BOF, the orientation image must be obtained. The orientation image shows the orientation of ridges and valleys in each pixel of the fingerprint image. Orientation image at each point (x, y) can be calculated using the following formula [21]

$$\begin{aligned} \text{angle}(x, y) &= \frac{\pi}{2} + \frac{1}{2} \tan^{-1} \left(\frac{\sum_{u=x-w/2}^{x+w/2} \sum_{v=y-w/2}^{y+w/2} 2G_x(u, v)G_y(u, v)}{\sum_{u=x-w/2}^{x+w/2} \sum_{v=y-w/2}^{y+w/2} (G_x(u, v)^2 - G_y(u, v)^2)} \right), \end{aligned} \quad (1)$$

where $w \times w$ is the size of window used for orientation calculation at point (x, y) , $G_x(u, v)$ and $G_y(u, v)$ are the local gradient in direction x and y , respectively, obtained using Sobel method. If the fingerprint image size is $M \times N$, then $1 \leq x \leq M$ and $1 \leq y \leq N$. Each orientation is changed to the nearest fundamental orientation. The fundamental orientations used for this research are

$$\theta_k = (k - 1) \frac{\pi}{16}, \quad k = 1, 2, \dots, 16. \quad (2)$$

Each fundamental orientation differs from the next by $\pi/16 = 11.25^\circ$ and covers orientations $\theta_k - \pi/32$ to $\theta_k + \pi/32$. In order to obtain BOF, orientation image is divided into square block of size $w \times w$ and the dominant orientation of pixels is extracted.

In the proposed method, since it is necessary for BOF to be rotated with a multiple of $\pi/16$, the orientation image is initially rotated and then the value of each pixel of orientation image is modified by the amount of rotation. Let θ_k be the value of a pixel of fingerprint orientation image at position (x, y) . To rotate the orientation image by $\Delta\theta = (\Delta k)(\pi/16)$, the result will be $\theta_{k'}$ at position (x', y') :

$$\theta_{k'} = \theta_k + \Delta\theta, \quad (3)$$

where $k' = \text{Mod}(k + \Delta k, 16)$ is the remainder of division of $k + \Delta k$ by 16, (x', y') is the point obtained from rotating (x, y) by $\Delta\theta$ and $\Delta k = 16(\Delta\theta/\pi)$.

For the next step, the rotated orientation image is changed to the relevant BOF.

Let f_q be the block orientation image of fingerprint q and let $f_{p, \Delta\theta_m}$ be the block orientation of fingerprint p rotated by $\Delta\theta_m$. Then the initial guess for the similarity of BOFs is

$$S'_{p,q,\Delta\theta_m} = \text{Max}_{x_1, y_1} \left(\sum_{x, y} \left\{ \delta[f_{p, \Delta\theta_m}(x + x_1, y + y_1) - f_q(x, y)] \right\} \right). \quad (4)$$

Function δ is one when its argument is zero and it is zero otherwise. Equation (4) expresses the similarity between fingerprints q and p , when p is rotated by $\Delta\theta_m$, which can be measured as follows.

- (i) BOF of one fingerprint ($f_{p, \Delta\theta_m}$) is shifted vertically and horizontally relative to that of other fingerprint (f_q).
- (ii) In each translation, the number of overlapping blocks with the same orientation is counted.

- (iii) Among all values of translations, maximum number of overlapping blocks with the same orientation gives the similarity of two BOFs.

The accuracy of this registration algorithm along the horizontal and vertical shifts is $\pm w/2$, where $w \times w$ is the block size of the orientation image.

In order to increase the similarity measure of BOFs, we normalize the similarity:

$$S'_{N_{p,q,\Delta\theta_m}} = \frac{S'_{p,q,\Delta\theta_m}}{N_{ov}}, \quad (5)$$

where N_{ov} is the overlapping region of two BOFs with the value of translation that gives $S'_{p,q,\Delta\theta_m}$.

Next, we obtain BOF from an orientation field image when the origin is shifted by $w/2$. As a result, 4 BOFs are obtained from each orientation field image (including cases with no translation, horizontal translation, vertical translation, and both). Let the similarity in each case be $S'_{N_{p,q,\Delta\theta_m,i}}$ where i shows each case of calculating BOF obtained from the translated orientation image for fingerprint p . Then, we can write

$$S'_{N_{p,q,\Delta\theta_m}} = \text{Max}_i (S'_{N_{p,q,\Delta\theta_m,i}}). \quad (6)$$

Calculating $S'_{N_{p,q,\Delta\theta_m,i}}$ for the case i needs the translation of two BOFs. However, the obtained translation for the case i , that gives $S'_{N_{p,q,\Delta\theta_m,i}}$, is slightly different from other cases. This point reveals that making these BOFs and similarity measuring from (6) has negligible effect on similarity calculation speed. This means that the similarity may be calculated from (4) (case of no translation for origin) and for other cases, the translation values differ a bit relative to the first case. As a result, the translation values for other cases are biased around that of the first case.

In order to improve the similarity criterion defined by (4), let A be the overlapping region that gives $S'_{N_{p,q,\Delta\theta_m}}$. In region A , we define a matrix b' with the same size as A , where the values of b' for overlapping blocks with the same orientation of two BOFs is 1 and 0 otherwise. Then, for the purpose of increasing similarity of images from the same fingerprint and reducing the similarity for the images from different fingerprints, we can define

$$b(x, y) = \begin{cases} 1, & \sum_{x_1, y_1 \in \{-1, 0, 1\}} b'(x - x_1, y - y_1) \geq t, \\ 0, & \text{otherwise,} \end{cases} \quad (7)$$

where t is a suitable threshold value. In this research, $t = 5$ is selected which means applying median filter on binary image b' . An improved measure of similarity can be expressed using the following formula:

$$S_{N_{p,q,\Delta\theta_m}} = \frac{\sum_{x,y} b(x, y)}{N_{ov}}. \quad (8)$$

We have measured the similarity based on overlapping blocks with identical orientation so far. Now, we aim to measure the

similarity based on the values for the orientation difference in unequal orientation overlapping blocks. To fulfill this, assume that the orientations of two BOFs at point (x, y) in the overlapping region A be θ_k and θ_j . Let us define orientation difference as

$$\text{ori_diff}(x, y) = \text{Min} \{ |\theta_k - \theta_j|, \pi - |\theta_k - \theta_j| \}. \quad (9)$$

Equation (9) demonstrates that the orientation difference of two blocks in position (x, y) is obtained such that the difference is always between 0 and 90° . We can define

$$d_{N_{p,q,\Delta\theta_m}} = \frac{\sum_{(x,y) \in \text{overlapping region A}} \text{ori_diff}(x, y)}{N_d}, \quad (10)$$

where

$$N_d = \frac{\pi}{2} \left(N_{ov} - \sum_{x,y} b(x, y) \right), \quad (11)$$

N_d , defined in (11), is used for normalization purpose. We are now in a position to define a new and combinational measure for similarity as

$$\text{Sori}_{p,q,\Delta\theta_m} = \alpha S_{N_{p,q,\Delta\theta_m}} + (1 - \alpha)(1 - d_{N_{p,q,\Delta\theta_m}}), \quad (12)$$

where α is the fusion coefficient and shows the contribution of each factor in fusion. These factors include identical orientation overlapping blocks (α and $S_{N_{p,q,\Delta\theta_m}}$) and unequal orientation overlapping blocks ($1 - \alpha$ and $1 - d_{N_{p,q,\Delta\theta_m}}$). Finally, a relation for the similarity of two fingerprints is given by

$$S = \text{Max}_{\Delta\theta_m} (\text{Sori}_{p,q,\Delta\theta_m}), \quad (13)$$

where

$$\Delta\theta_m \in \left\{ \frac{m\pi}{16} \mid m = -n, -n + 1, \dots, n - 1, n \right\}. \quad (14)$$

As a result, the permissible relative rotation of the two fingerprints is $\pm n\pi/16$, the accuracy of registration algorithm in horizontal and vertical direction is $\pm w/4$, and the relevant accuracy for rotation angle is $\pm\pi/32 = \pm 5.625^\circ$. The shift values and rotation angle for which the similarity is obtained by (13) give the registration parameters of two fingerprint images. We use these parameters for the registration of fingerprints for texture-based similarity measuring developed in subsequent section.

When similarity measure given by (13) is greater than a threshold, the two fingerprint images are supposed to be the same. The block diagram of proposed orientation-based fingerprint similarity measure is shown in Figure 1.

At first glance, it seems that an exhaustive and possibly time-consuming search may be needed for calculating the

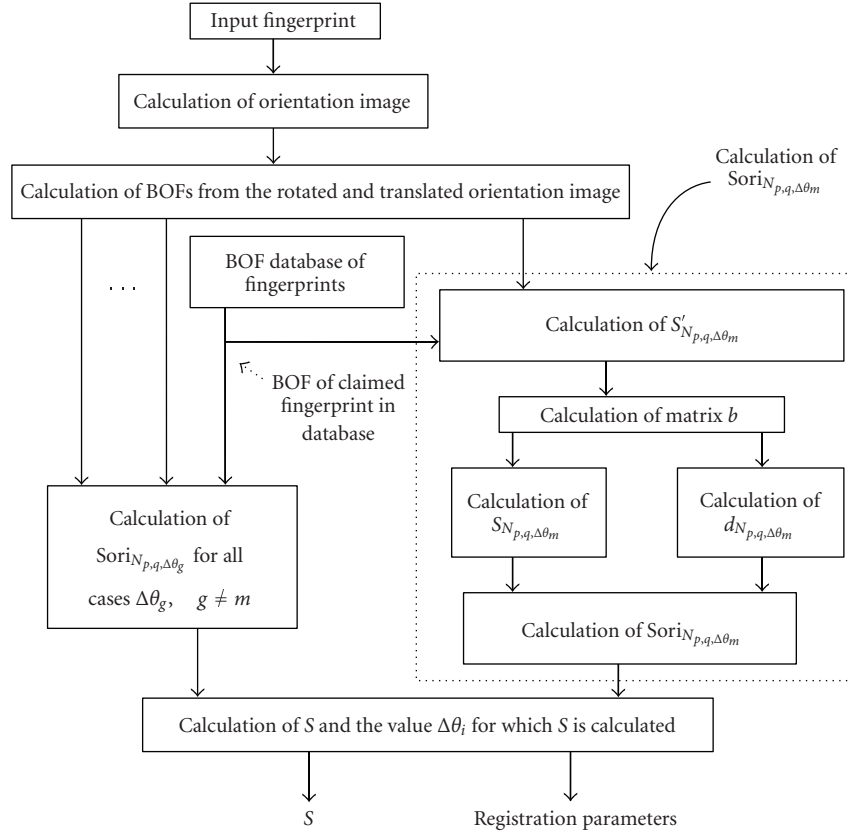


FIGURE 1: Block diagram of proposed orientation-based fingerprint similarity measure.

similarity of two fingerprint images and registration parameters using the proposed approach. However, there are points to speed up the search as follows.

- (i) The variation interval of horizontal and vertical translations, which is used in (4), are usually restricted to $\pm 1/2$ of number of horizontal and vertical blocks. For example, for a 364×256 image with block size of 16×16 , the variations of translations along the vertical and horizontal axis are ± 11 and ± 7 , respectively.
- (ii) As mentioned earlier, biasing the translations for the case “(i)” relative to the previous case, (6), can reduce the computational complexity.
- (iii) If the relative rotation of fingerprint images is not very high, that is, less than 30° , the translation values for each rotation can be biased around that of the previous rotation. This results in significant improvement of similarity calculation speed.

It seems that the proposed approach is somewhat robust against nonlinear deformation and noise. The main reasons for this are the following.

- (i) The method is based on the orientation of blocks *not* the orientation of pixels.
- (ii) As the orientation is normalized to the nearest sixteen fundamental orientations, the effect of noise and

nonlinear deformation may be reduced. Moreover, unwanted orientation variation may cause the normalized orientations to be changed by a small amount and it has a positive effect on the similarity based on unequal orientation overlapping blocks (10).

However, if the image noise is reduced or methods for fingerprint image enhancement are employed to improve the ridge orientations, they may positively affect the proposed similarity measure.

There are a number of methods for calculating the orientation of fingerprint ridges [22]. In this paper, (1) is used for this purpose. However, (1) presents one way for calculating the orientation. No problem can be imagined with this algorithm if one calculates the orientation using other method. If another scheme calculates the orientations more accurately, it may cause the propose approach to give better similarity measure.

3. SIMILARITY MEASURING USING TEXTURE FEATURES

In order to extract texture features, Gabor filter bank are applied on the fingerprint image. Gabor filter bank usually includes 8 filters in 8 directions that cover equally spaced orientations between 0 and 180° . An even type of a Gabor filter

in space domain is given by

$$g(x', y', \theta, f) = \exp\left(-\frac{x'^2}{2\sigma_x^2} - \frac{y'^2}{2\sigma_y^2}\right) \cos(2\pi f x'). \quad (15)$$

If (x, y) is a point of an image, (x', y') will be obtained by

$$\begin{aligned} x' &= x \cos \theta + y \sin \theta, \\ y' &= -x \sin \theta + y \cos \theta, \end{aligned} \quad (16)$$

where θ is Gabor filter angle and f is the frequency of ridges and equals to the inverse of average distance of parallel ridges.

The procedure for distance measuring of two fingerprints (input and template) based on texture features is as follows.

- (A) The input fingerprint is registered relative to template using the parameters obtained in previous section for registration.
- (B) The input fingerprint is normalized with a constant mean and variance for grey-level values. Let $I(x, y)$, M_0 , and Var_0 be grey level at position (x, y) , mean, and variance of input fingerprint image, respectively. Then, the formula for normalization is given by

$$f(x, y) = \begin{cases} M_0 + \sqrt{\frac{\text{Var}_0 (I(x, y) - M)^2}{\text{Var}}}, & \text{if } I(x, y) > M, \\ M_0 - \sqrt{\frac{\text{Var}_0 (I(x, y) - M)^2}{\text{Var}}}, & \text{otherwise,} \end{cases} \quad (17)$$

where $f(x, y)$, M , and Var are the grey level, constant mean, and variance of normalized image, respectively.

- (C) The filter bank is applied on input fingerprint and 8 output images are obtained.
- (D) The obtained images are divided into square blocks and absolute average deviation from the mean (AAD) for each block is extracted. The feature vector includes AADs of all blocks of all images. A typical fingerprint with its filtered images and extracted features are shown in Figure 2.
- (E) The Euclidean distance between the input feature vector and that of the template is used for distance measure of fingerprint images. The less distance, the more similarity.

Steps (B) to (D) are also followed for each fingerprint in offline template construction (enrollment).

Similar procedure is used in [16]. However, in [16] the registration of fingerprint images is achieved using minutiae features unlike the proposed method that utilizes orientation field for fingerprints registration.

4. SIMILARITY MEASURING USING SPECTRAL FEATURES

The magnitude of two-dimensional Fourier Transform of a fingerprint image is called spectrum. In order to extract feature from spectrum, the image is first normalized with a constant mean and variance for its grey-level values. Then,

spectrum of the image is calculated. Because of the central symmetry property of spectrum, only the right half-plane of spectrum is used for feature extraction. In addition, the features are extracted only from frequency intervals $[0 \ \pi/2]$ along the horizontal frequency axis and $[-\pi/2 \ \pi/2]$ along the vertical frequency axis because there is insignificant information out of these intervals. The area restricted to the mentioned intervals is divided into rectangular blocks; and for each block, the mean of spectrum values is calculated and labeled as an element of spectral feature vector. In addition, it is appropriate for frequency block dimensions along horizontal and vertical axis to be the same. On the other hand, since the image lengths in x and y directions may be unequal, a rectangular block, instead of square block, may be selected for feature extraction. The resulting feature vector is image translation invariant. It is extracted and stored in database. In addition, the spectrum of input fingerprint is rotated in steps of 11.25° (clockwise and counter clockwise). For each step, a feature vector is extracted. The criterion for fingerprint verification is given by

$$d_{\text{spec}} = \text{Min}_{\Delta\theta_i} (d_{\Delta\theta_i}), \quad (18)$$

$$\Delta\theta_i \in \left\{ \frac{i\pi}{16} \mid i = -n, -n+1, \dots, n \right\}, \quad (19)$$

where $d_{\Delta\theta_i}$ is Euclidean distance between the input image feature vector and the template when the spectrum of input image rotated by $\Delta\theta_i$. The two fingerprints are assumed to be the same if d_{spec} is less than a threshold.

5. SIMILARITY MEASURE NORMALIZATION

Decision-level fusion of measures defined in Sections 2 through 4 needs a normalization step to be applied on each measure, as it is intended to use sum of similarity scores for fusion. There are several normalization methods like *z-score*, *MAD*, *min-max*, and *tanh*. We select *tanh* normalization method since it is efficient and robust against outliers [23]. The related formula for *tanh* normalization method is given by

$$s'_k = \frac{1}{2} \left\{ \tanh \left(k \left(\frac{s_k - \mu_{GH}}{\sigma_{GH}} \right) \right) + 1 \right\}, \quad (20)$$

where s'_k is normalized *similarity* or *distance* score. μ_{GH} and σ_{GH} are the mean and standard deviation estimates, respectively, of genuine score distribution as given by Hampel estimators [23], and k is a suitable constant. The distance to similarity transformation is achieved by subtracting the normalized scores by 1 so that all normalized scores are of similarity type.

6. EXPERIMENTS AND DISCUSSION

The experimental results presented in this section are divided into 3 parts. The first part details experiments on proposed orientation-based method. The second part compares the proposed method with FingerCode-based method [7]. The third part evaluates fusion of proposed nonminutiae-based fingerprint verification systems.

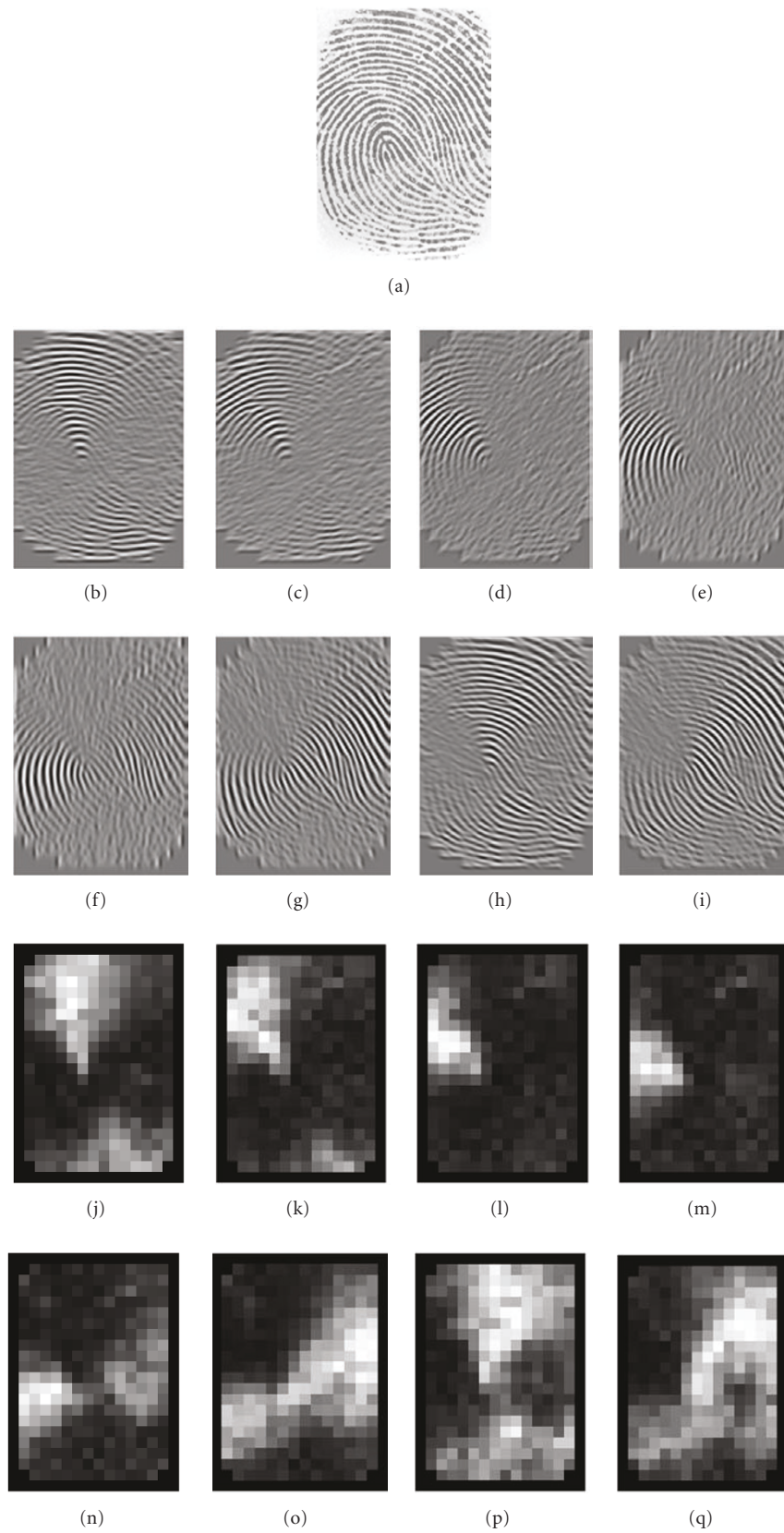


FIGURE 2: A typical fingerprint with its filtered images and extracted features.

We have selected *FVC2000 DB2 Set-A* [24] database for evaluation of the verification systems developed in previous sections. This database includes 800 fingerprint images from 100 individuals, each having eight impressions. Images are acquired using a capacitive scanner with size 364×256 .

6.1. Orientation-based similarity evaluation

In order to evaluate the proposed similarity criterion based on orientation field, we have setup several experiments. Before BOF extraction, segmentation on the image is achieved to separate foreground from background. BOF is extracted only from foreground region. The relative rotation angle of the images is selected to be 22.5° (14). Initially, the first impression of each fingerprint is selected and its BOF with the block size 16×16 is extracted and stored in database. The similarities of each of the remaining impressions of fingerprint images (700 images) with all 100 BOFs in database are calculated. We sort the images in database in descending order according to the similarity with each input fingerprint. Let the maximum allowable fingerprints in database that can be searched to find a match with input fingerprint be the first p images. We search the first p image to find a match with input fingerprint. If n is the number of fingerprints in database (here 100), penetration rate is defined as [22]

$$\text{Penet_rate} = \frac{p}{n}. \quad (21)$$

Penetration rate determines the maximum number of images to be searched in database to find a match with input fingerprint. With increasing penetration rate, a match in database can be found for more input fingerprints. Also, for a fixed penetration rate, the similarity algorithm that give a match for more input fingerprints in the first p image in database has better similarity criterion. Moreover, it has better distinctiveness property between two different fingerprint images.

Figure 3 shows percent of input fingerprints for which a match cannot be found in the first p fingerprint in database (when the database is sorted in descending order according to similarity criterion to each input fingerprint) versus penetration rate. There are 2 plots in this figure. One plot is for $\alpha = 1$ which means the similarity of BOFs only when only equal orientation overlapping blocks is considered. The other is for $\alpha = 0.5$ meaning the same contribution for identical orientation overlapping blocks as for unequal orientation overlapping blocks, in similarity measuring of BOFs. This figure shows that using unequal orientation overlapping blocks has considerable performance improvement.

If the images in database are sorted in descending order according to similarity criterion to each input fingerprint, the average number of the images in database that must be searched to find a match for each input fingerprint is called average penetration [22]. Figure 4 shows average penetration versus fusion coefficient, α (see (12)). As the average penetration decreases, performance of similarity criterion increases. The figure shows the best performance has been obtained for values $0.4 \leq \alpha \leq 0.5$.

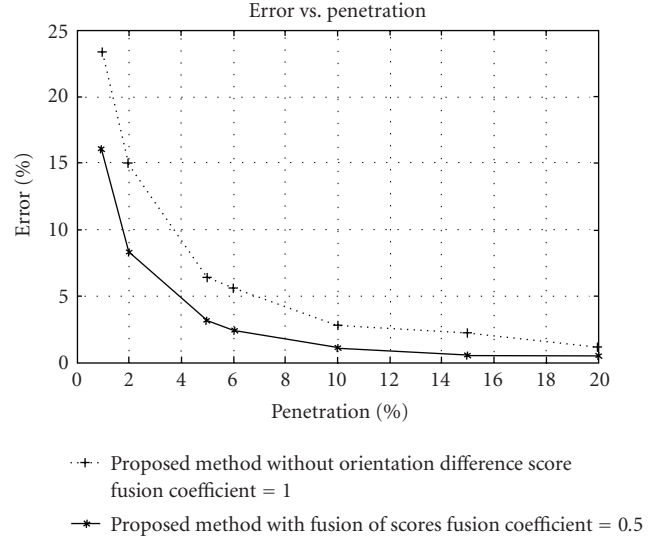


FIGURE 3: Percent of input fingerprints for which a match cannot be found in the first p fingerprint in database (producing error) versus penetration rate. One plot is for $\alpha = 1$ and the other is for $\alpha = 0.5$.

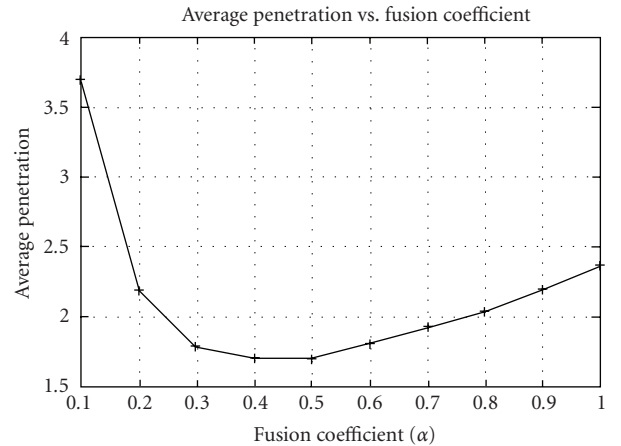


FIGURE 4: Average penetration versus fusion coefficient (α).

6.2. Orientation-based similarity measure versus FingerCode

We have made a comparison between the orientation-based fingerprint similarity measure proposed in Section 2 and FingerCode similarity measure [7]. FingerCode of a fingerprint image can be computed as follows.

- (i) The image is normalized with a constant mean and variance for its grey-level values.
- (ii) The core point of fingerprint is extracted.
- (iii) 8 Gabor filters are applied on fingerprint image and 8 output images are extracted.
- (iv) The output image is divided into predefined sectors around the core point and for each sector, the absolute

average deviation from the mean (AAD) is extracted and labeled as an element of FingerCode feature vector.

A fingerprint image with its FingerCode feature vector is shown in Figure 5. The Euclidean distance of relevant FingerCodes of 2 fingerprints shows the similarity of two fingerprints. The less distance, the more similarity.

In order to extract FingerCode from each fingerprint, we initially detect the core point using [21]. All detected core points are manually checked; as it is possible for core point to be erroneously located. Approximately, 1% of test fingerprints do not have a core point in a suitable position for FingerCode extraction [16] and hence, they are rejected. The filter size is 33×33 and parameters for (15) are $\sigma_x = \sigma_y = 4$ and $f = 0.125$. Also, the length of each sector along the radial direction is 20 pixels. According to Figure 5 and selecting 16 sectors for each circle, 48 features are extracted for each Gabor filter direction. In total, there must be 384 features extracted for a fingerprint image.

The same procedure used in the previous subsection for obtaining the curves in Figure 3 is now followed for FingerCode-based method. However, the similarity based on orientation is substituted by the similarity based on FingerCodes.

The proposed orientation-based similarity algorithm is compared with FingerCode method in Figure 6. This figure shows percent of input fingerprints for which a match cannot be found in the first p fingerprint in database (when the database is sorted in descending order according to similarity criterion to each input fingerprint) versus penetration rate. According to this figure, orientation-based method outperforms FingerCode method. Thus, the proposed method works well for defining similarity between the same fingerprints and distinctiveness between different fingerprints. Also, in Table 1, comparisons between different specifications of the mentioned methods are made. The proposed method is slightly better than FingerCode-based method in terms of speed and number of extracted features. The points mentioned in Section 2 to speed up the proposed approach make it faster than FingerCode-approach. The most similar fingerprint in database, according to FingerCode-based method, will be the match fingerprint. This, of course, holds true with only 62% of input fingerprints. Therefore, recognition rate for FingerCode-based method is 62%. Our proposed method has a significant improvement for this parameter (84%).

Besides, the proposed method does not need core point despite the FingerCode method. The core point may not be detected accurately or located in a suitable position for FingerCode extraction.

6.3. Nonminutiae-based fusion

In this section, we aim to fuse decision-level fusion of orientation, textural, and spectral information of fingerprint images. For BOF-based similarity measurement method proposed in Section 2, the first impression of each fingerprint is selected and its BOF is extracted and stored in database



FIGURE 5: A fingerprint and its extracted FingerCode features around the core point.

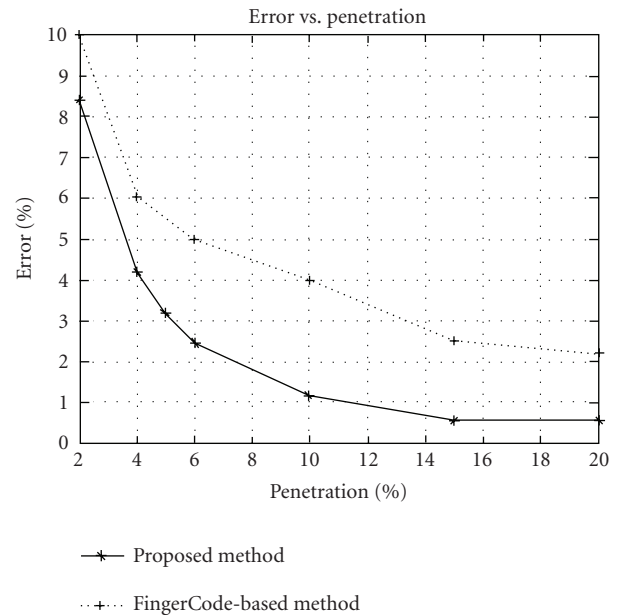


FIGURE 6: Percent of input fingerprints for which a match cannot be found in the first p fingerprint in database (producing errors) versus penetration rate. Two curves are shown in this figure, one for proposed method and the other for FingerCode-based method.

for template construction. Implementation considerations of this method are presented in Section 6.1. Also, $\alpha = 0.5$ is selected for (12).

For feature extraction proposed in Section 3, filtered fingerprint images are divided into 16×16 blocks and features are extracted. The filter size is 33×33 and parameters for (15) are $\sigma_x = \sigma_y = 4$ and $f = 0.125$.

Since the fingerprint image size is 364×256 , as explained in Section 4, rectangular blocks with size 16×11 are selected for spectral feature extraction. Also, to increase the verification accuracy, the first two impressions of the same fingerprint are chosen and the mean of associated registered

TABLE 1: Specifications of proposed BOF-based similarity measure and FingerCode.

Method	No. of features	Time (feature extraction and each similarity measuring)*	Recognition rate (%)	Average penetration
Proposed BOF-based	352	1.5 s	84	1.72
FingerCode	384	1.8 s	62	2.4

*Implemented using a 2 GHz computer with 256 Mbytes RAM and MATLAB 7.0 software.

spectral feature vectors is obtained and stored in database for template construction.

Similarity measure in each method is normalized according to (20). If the measured score is of distance type, the normalized score is subtracted from 1. *FVC2000 DB2 Set-B* database is used to estimate the normalization parameters in (20).

The remaining six impressions of each fingerprint that do not take part in template construction are used to make 600 genuine attempts. Also, each fingerprint is chosen and all 2nd impression of other fingerprints makes the false attempts for the selected fingerprint. As a result, a total of 9900 false attempts are contemplated for all fingerprints in database.

Receiver operating characteristic (ROC) curve shows false acceptance rate (FAR) versus false rejection rate (FRR) for different threshold values. The ROC curves of three methods of similarity measuring including orientation, texture, and spectrum are shown in Figure 7. Also, ROC curve for decision-level fusion of mentioned methods is shown in this figure. The fusion method is based on sum rule of normalized scores. This ROC curve shows improvement when using decision-level fusion compared with each method. Spectral-based feature method has lower performance than the other methods which means that the distinctiveness of spectral features is less than orientation or texture-features. For low values of FAR, texture-based method is better than orientation-based method. The opposite statement is true for low values of FRR.

ROC curves for the decision-level fusion of different kind of features are shown in Figure 8. The 3-feature-based fusion outperforms each combination of 2-feature-based fusion method. Fusion of orientation and spectrum has approximately the same performance as 3-feature method only for low values of FRR.

Density distribution functions of genuine and impostor attempts for 3-feature based fusion method are shown in Figure 9. To obtain these curves, the following formulas are used:

$$p(s | \text{Genuine}) = \left. \frac{dFRR(t)}{dt} \right|_{t=s}, \quad (22)$$

$$p(s | \text{Impostor}) = - \left. \frac{dFAR(t)}{dt} \right|_{t=s},$$

where t is the threshold value for which FAR and FRR are computed. Decidability index (DI) for a biometric verifica-

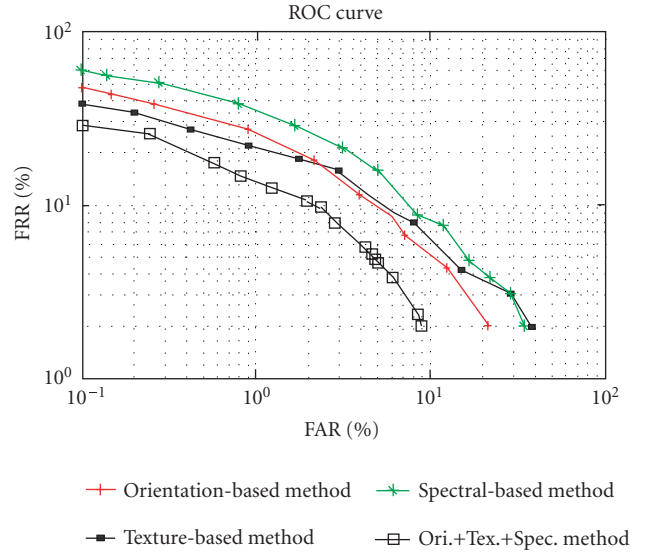


FIGURE 7: ROC curve for three proposed verification method and decision-level fusion of them.

tion system is given by

$$DI = \frac{|\mu_I - \mu_G|}{\sqrt{(\sigma_I^2 + \sigma_G^2)/2}}, \quad (23)$$

where μ_G and σ_G are the mean and standard deviation of genuine attempts, respectively, and μ_I and σ_I are the mean and standard deviation of impostor attempts, respectively. The system capability to distinguish between impostor and genuine attempts can be improved by increasing DI . Another important parameter for comparing verification systems is EER (equal error rate) which occurs when $FAR = FRR = EER$. In Table 2, different specifications of proposed verification systems are compared. The number of features stored in database per fingerprint for each method is shown in this table. Verification speeds of methods are also compared in this table. Verification algorithms are implemented using a 2 GHz computer with 256 Mbytes RAM and MATLAB 7.0 software. The reported time includes feature extraction from input fingerprint plus matching with claimed fingerprint in database. Different performance indexes for decision-level fusion of verification methods are presented in Table 3. The fusion of 3-feature-based method outperforms other methods in terms of EER and DI . Although EER of 3-feature based fusion method is near the fusion of orientation and spectrum, the former has considerable improvement

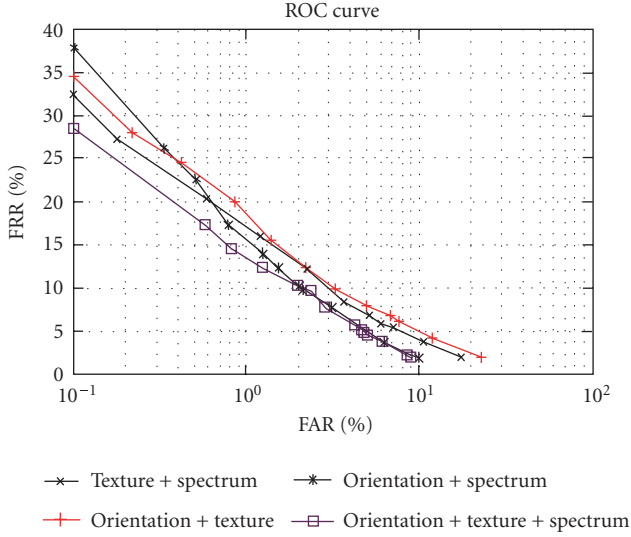


FIGURE 8: ROC curve for the decision-level fusion of features.

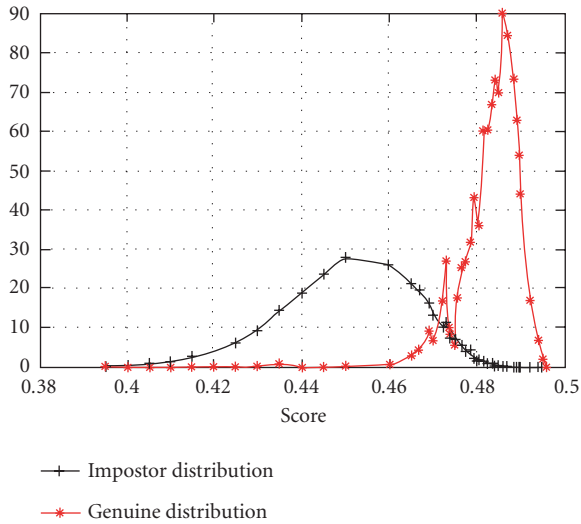


FIGURE 9: Density functions of impostor and genuine distributions for fusion of 3-feature extraction methods.

at low values of FAR compared with the latter, as shown in Figure 8. *Orientation-plus-spectrum* fusion has better performance than *orientation-plus-texture* fusion method. The extraction of texture features is accomplished in different orientations and hence, there is a correlation between orientation and texture features. Fixed rule fusion methods, unlike trainable ones, has low performance for the case of dependent features. In addition, spectral and orientation features extraction are achieved through independent methods. Orientation-based registration algorithm is the starting point for the extraction of texture features from an input image. Therefore, the errors that occur for similarity measuring on orientation domain are propagated to texture feature extraction from input image. It causes *orientation-plus-*

TABLE 2: Performance indexes for nonminutiae-based verification methods.

Method	No. of features	EER (%)	Verification time (s)*	DI
Orientation	352	6.90	1.5	2.7070
Texture	8×280	8.10	1.8	2.6884
Spectrum	72	8.86	0.5	2.6350

* Verification algorithms are implemented using MATLAB 7.0 software.

TABLE 3: Performance indexes for decision-level fusion of verification methods.

Method	EER (%)	DI
Orientation + Texture	5.90	2.9596
Orientation + Spectrum	5.09	3.1905
Texture + Spectrum	6.84	3.1498
Orientation + Texture + Spectrum	4.83	3.4673

spectrum fusion method to have better performance indexes than *texture-plus-spectrum* fusion method.

7. CONCLUSION

In this study, three methods for fingerprint verification-based on nonminutiae features have been proposed and compared. The proposed methods are based on orientation, texture, and spectrum of fingerprint images. None of the suggested methods need core point detection stage. In addition, they are translation and rotation invariant. Compared with FingerCode similarity measure, the proposed orientation-based similarity measure is of better performance. Then, the similarity in each method was normalized and decision-level information fusion of the proposed methods was examined. It was observed that the fusion of all three methods had better performance than each method or each combination of the two methods. Trainable fusion methods may have better performance than fixed rule fusion methods. This point will be considered in the future work. In addition, if nonminutiae proposed methods are fused with minutiae-based methods, it may result in considerable performance improvement for minutiae-based fingerprint verification of low-quality images.

ACKNOWLEDGMENT

The authors would like to thank the Iran Telecommunication Research Center (ITRC) for funding this research as Project 500/8229.

REFERENCES

- [1] X. Tong, J. Huang, X. Tang, and D. Shi, "Fingerprint minutiae matching using the adjacent feature vector," *Pattern Recognition Letters*, vol. 26, no. 9, pp. 1337–1345, 2005.
- [2] E. Zhu, J. Yin, and G. Zhang, "Fingerprint matching based on global alignment of multiple reference minutiae," *Pattern Recognition*, vol. 38, no. 10, pp. 1685–1694, 2005.

- [3] M. Tico and P. Kuosmanen, "Fingerprint matching using an orientation-based minutia descriptor," *IEEE Transactions on Pattern Analysis and Machine Intelligence*, vol. 25, no. 8, pp. 1009–1014, 2003.
- [4] H. Ghassemian, "A robust on-line restoration algorithm for fingerprint segmentation," in *Proceedings of IEEE International Conference on Image Processing (ICIP '96)*, vol. 2, pp. 181–184, Lausanne, Switzerland, September 1996.
- [5] C.-T. Hsieh, E. Lai, and Y.-C. Wang, "An effective algorithm for fingerprint image enhancement based on wavelet transform," *Pattern Recognition*, vol. 36, no. 2, pp. 303–312, 2003.
- [6] M. Tico, P. Kuosmanen, and J. Saarinen, "Wavelet domain features for fingerprint recognition," *Electronics Letters*, vol. 37, no. 1, pp. 21–22, 2001.
- [7] A. K. Jain, S. Prabhakar, L. Hong, and S. Pankanti, "Filter bank-based fingerprint matching," *IEEE Transactions on Image Processing*, vol. 9, no. 5, pp. 846–859, 2000.
- [8] C.-J. Lee and S.-D. Wang, "Fingerprint feature extraction using Gabor filters," *Electronics Letters*, vol. 35, no. 2–4, pp. 288–290, 1999.
- [9] C.-J. Lee and S.-D. Wang, "Fingerprint feature reduction by principal Gabor basis function," *Pattern Recognition*, vol. 34, no. 11, pp. 2245–2248, 2001.
- [10] C.-H. Park, J.-J. Lee, M. J. T. Smith, S.-I. Park, and K.-H. Park, "Directional filter bank-based fingerprint feature extraction and matching," *IEEE Transactions on Circuits and Systems for Video Technology*, vol. 14, no. 1, pp. 74–85, 2004.
- [11] A. M. Bazen, G. T. B. Verwaaijen, S. H. Gerez, L. P. J. Veenturf, and B. J. Van Der Zwaag, "A correlation-based fingerprint verification system," in *Proceedings of 11th Annual Workshop on Circuits, Systems and Signal Processing (ProRISC '00)*, pp. 205–213, Veldhoven, The Netherlands, November–December 2000.
- [12] A. T. B. Jin, D. N. C. Ling, and O. T. Song, "An efficient fingerprint verification system using integrated wavelet and Fourier-Mellin invariant transform," *Image and Vision Computing*, vol. 22, no. 6, pp. 503–513, 2004.
- [13] V. A. Sujana and M. P. Mulqueen, "Fingerprint identification using space invariant transforms," *Pattern Recognition Letters*, vol. 23, no. 5, pp. 609–619, 2002.
- [14] J. Gu, J. Zhou, and D. Zhang, "A combination model for orientation field of fingerprints," *Pattern Recognition*, vol. 37, no. 3, pp. 543–553, 2004.
- [15] N. Yager and A. Amin, "Evaluation of fingerprint orientation field registration algorithms," in *Proceedings of the 17th International Conference on Pattern Recognition (ICPR '04)*, vol. 4, pp. 641–644, Cambridge, UK, August 2004.
- [16] A. Ross, A. K. Jain, and J. Reisman, "A hybrid fingerprint matcher," *Pattern Recognition*, vol. 36, no. 7, pp. 1661–1673, 2003.
- [17] S. Prabhakar and A. K. Jain, "Decision-level fusion in fingerprint verification," *Pattern Recognition*, vol. 35, no. 4, pp. 861–874, 2002.
- [18] G. L. Marcialis and F. Roli, "Fusion of multiple fingerprint matchers by single-layer perceptron with class-separation loss function," *Pattern Recognition Letters*, vol. 26, no. 12, pp. 1830–1839, 2005.
- [19] J. Qi, S. Yang, and Y. Wang, "Fingerprint matching combining the global orientation field with minutia," *Pattern Recognition Letters*, vol. 26, no. 15, pp. 2424–2430, 2005.
- [20] G. L. Marcialis and F. Roli, "Fingerprint verification by decision-level fusion of optical and capacitive sensors," *Pattern Recognition Letters*, vol. 25, no. 11, pp. 1315–1322, 2004.
- [21] A. M. Bazen and S. H. Gerez, "Systematic methods for the computation of the directional fields and singular points of fingerprints," *IEEE Transactions on Pattern Analysis and Machine Intelligence*, vol. 24, no. 7, pp. 905–919, 2002.
- [22] D. Maltoni, D. Maio, A. K. Jain, and S. Prabhakar, *Hand Book of Fingerprint Recognition*, Springer, New York, NY, USA, 2003.
- [23] A. K. Jain, K. Nandakumar, and A. Ross, "Score normalization in multimodal biometric systems," *Pattern Recognition*, vol. 38, no. 12, pp. 2270–2285, 2005.
- [24] D. Maio, D. Maltoni, R. Cappelli, J. L. Wayman, and A. K. Jain, "FVC2000: fingerprint verification competition," *IEEE Transactions on Pattern Analysis and Machine Intelligence*, vol. 24, no. 3, pp. 402–412, 2002.

Sadegh Helfroush was born in Iran, in 1970. He received his B.S. degree and M.S. degree in electrical engineering from Shiraz University, Shiraz, Iran, in 1992, and Sharif University of Technology, Tehran, Iran, in 1994, respectively. He is currently Ph.D. student in communication engineering at Tarbiat Modares University, Tehran, Iran. His major fields of interest are pattern recognition, image processing, neural networks, machine vision, and biometrics.



Hassan Ghassemian was born in Iran, in 1956. He received the B.S.E.E. degree from Tehran College of Telecommunication, in 1980, and the M.S.E.E. and Ph.D. degrees from Purdue University, West Lafayette, USA, in 1984 and 1988, respectively. He is a Professor of Electrical Engineering at Tarbiat Modares University, in Tehran, Iran. His research interests include multisource image processing and analysis, information processing and pattern recognition in remote sensing, and biomedical engineering. He is an IEEE Senior Member.

